MASTER'S THESIS OF NATURAL SCIENCE

Characterization of a DNAPL Contaminated Site by Partitioning Behavior of Noble Gas

February 2020

Graduate School of Seoul National University

College of Natural Science

School of Earth and Environmental Sciences

Ilryoung Cho

ABSTRACT

Among partitioning tracers, noble gases are characterized by their biochemical inertness, providing an opportunity to identify the physical fractionation processes in the subsurface system. Thus, noble gases are often used to describe systems of oil and natural gas reservoirs. Taking advantage of the features mentioned above, this study applied noble gas in characterizing the TCE contaminated field which is known to be harmful to various systems in the human body. Groundwater is sampled at the site deeply studied in terms of TCE contamination to figure out whether noble gas is applicable in understanding TCE distribution through its partitioning pattern. By applying batch equilibrium and Rayleigh partitioning equations, noble gas tracers showed clear change depending on TCE distribution and seasonal variations. It was also able to calculate the TCE/water ratio of the study site as 0.03–0.05. This study suggested that by using noble gas, it is able to identify the distribution of residual TCE considering the effect of seasonal water table fluctuation. Moreover, the partitioning ratio of TCE and groundwater could be acquired by understanding the behavior of noble gas.

Key Words: noble gas, TCE, partitioning, tracer, DNAPL, groundwater contamination

Table of Contents

List of Figures

List of Tables

1. INTRODUCTION

Trichloroethylene (TCE) is universally used as a degreasing agent (Russell et al., 1992) and recently one of the most pervasive chlorinated compounds corrupting groundwater among industrial solvents (Kao and Lei, 2000). TCE is a well-known carcinogen and shows toxicity to many other systems in the human body (Chiu et al., 2012) (Table 1-1). Therefore, the Environmental Protection Agency in the United States of America has set a standard for various types of groundwater. As for drinking water, the maximum contaminant level is 0.005 ppm, and 0.03 ppm for groundwater that can affect indoor vapor (Monosson, 2008).

To manage the TCE contaminated region, it is important to understand the degree and extent of the damage. According to Davis et al. (2002), traditional sampling methods were mainly direct sampling of water or soil. However, they were able to interrogate only a small volume of the aquifer as a representative which was insufficient for large scale contaminant regions (Davis et al., 2002). To overcome the disadvantage, there were some studies using partitioning tracers in terms of hexanol injection (Istok et al., 2002) or Rn push-pull test (Davis et al., 2002) that covers larger extent accurately to characterize the source and extent of TCE contamination (Young et al., 1999).

Among partitioning tracers, noble gas is noticeable because sources of noble gases are relatively clear due to their chemical inertness. There are

primitive noble gases and radioactively generated noble gases (Ballentine and Burnard, 2002). Afterward, degassing, mixing and atmospheric loss brings change in abundance or isotopic compositions (Ballentine et al., 2002). Since there are no chemical processes involved, it is possible to interpret the fractionation or distribution of noble gas by only considering the physical changes like temperature, pressure and phase composition (Barry et al., 2017).

Considering this advantage, there were previous studies that used noble gas in oil or natural gas exploration. Barry et al. (2017) and Pinti and Marty (1995) used noble gas as a partitioning tracer to quantify the ratio of oil, gas, and water in the reservoir. Moreover, Zaikowski and Spangler (1990) used the changes in the noble gas composition to predict gas production at the natural gas reservoir. Despite the history of noble gas application in oil and natural gas industry, the noble gas method was rarely applied to understand the distribution of Non-Aqueous Phase Liquid (NAPL) contamination (i.e. TCE) in groundwater. There was a lab-scale investigation conducted to evaluate the applicability of He and Ne as partitioning tracers for finding and quantifying TCE and PCE contamination at water-saturated sand columns. However, it ended after leaving the limitation of only providing a basis for field-scale application (Divine et al., 2003).

With the necessity for the field-scale experiments, this study was conducted at the test site in Road Administrative Office (RAO), Wonju,

Korea with massive TCE contamination from the past. This site is deeply studied with dual-isotope data, radon concentration, microbial community and water-level fluctuation data to understand the TCE distribution (Kaown et al., 2014; Lee et al., 2015; Yang and Lee, 2012; Yang et al., 2012; Yang et al., 2014). In this study, the noble gas partitioning pattern between groundwater and TCE was examined by analyzing the noble gas concentrations together with TCE concentrations and the groundwater level. The purpose of this study is to figure out whether noble gas is appropriate in finding the source zone and estimating the degree of TCE contamination at the actual contaminated field. For further application of the partitioning nature, noble gas components were also related to seasonal variations due to water table fluctuation.

Table 1-1 Human health effects of TCE

Weight of evidence	Threatened tissue or organ system
Strong evidence (Human studies)	Central nervous system
	Kidney
	Immune system
	Reproductive system
	Fetal cardial formation
	Liver
Limited evidence (Relatively focused on animal studies)	Overall fetal formation
	Respiratory tract

2. STUDY AREA

2.1 Site description

The study area is located in Wonju, about 75 km east of the capital of the Republic of Korea, Seoul (Figure 2-1 (a)). The Woosan industrial complex (WIC) has been formed in Wonju since 1970, and at the western part of the WIC locates the RAO of Gangwon Province (Figure 2-1 (b), (c)). Previous researches found out that various reagents were used for the asphalt quality test starting from 1981. Even though the exact names and quantities of the discarded solvents are unidentified, TCE is known to be the main contaminant in the test region (Yang et al., 2012).

The aquifer at the study site is consisted of soil and alluvial deposits with highly fractured bedrock lying underneath (Baek and Lee, 2011, Yu et al., 2006). Figure 2-2 is a geological map of Wonju, and the study site is located in the Jurassic granite region.

In terms of hydrology, the study site shows water table fluctuation in accordance with seasonal change. Figure 2-3 shows the water table change and rainfall rate at RAO during the sampling period. Water level change data is from well KDMW1, KDPW2, 4, 7 logged by CTD Diver (CTD Diver, Eijkelkamp Soil & Water, Netherlands). Divers are installed at wells in the main source zone (KDMW1, KDPW2, KDPW4) and at well with no pavement (KDPW7) which is thought to show higher water level change

than wells located at the paved region. Water level monitored from all wells showed increase during the test period. Among 4 wells, KDPW7 showed the highest water table level fluctuation of 2.99 m from 96.98 (m, a.s.l.) to 99.27 (m, a.s.l.) and KDMW1 showed the least water table fluctuation of 1.14 m from 107.53 (m, a.s.l.) to 108.67 (m, a.s.l.). The water level increased with heavy rainfall from late August to early September 2018, and the increase rate dropped steadily until early October.

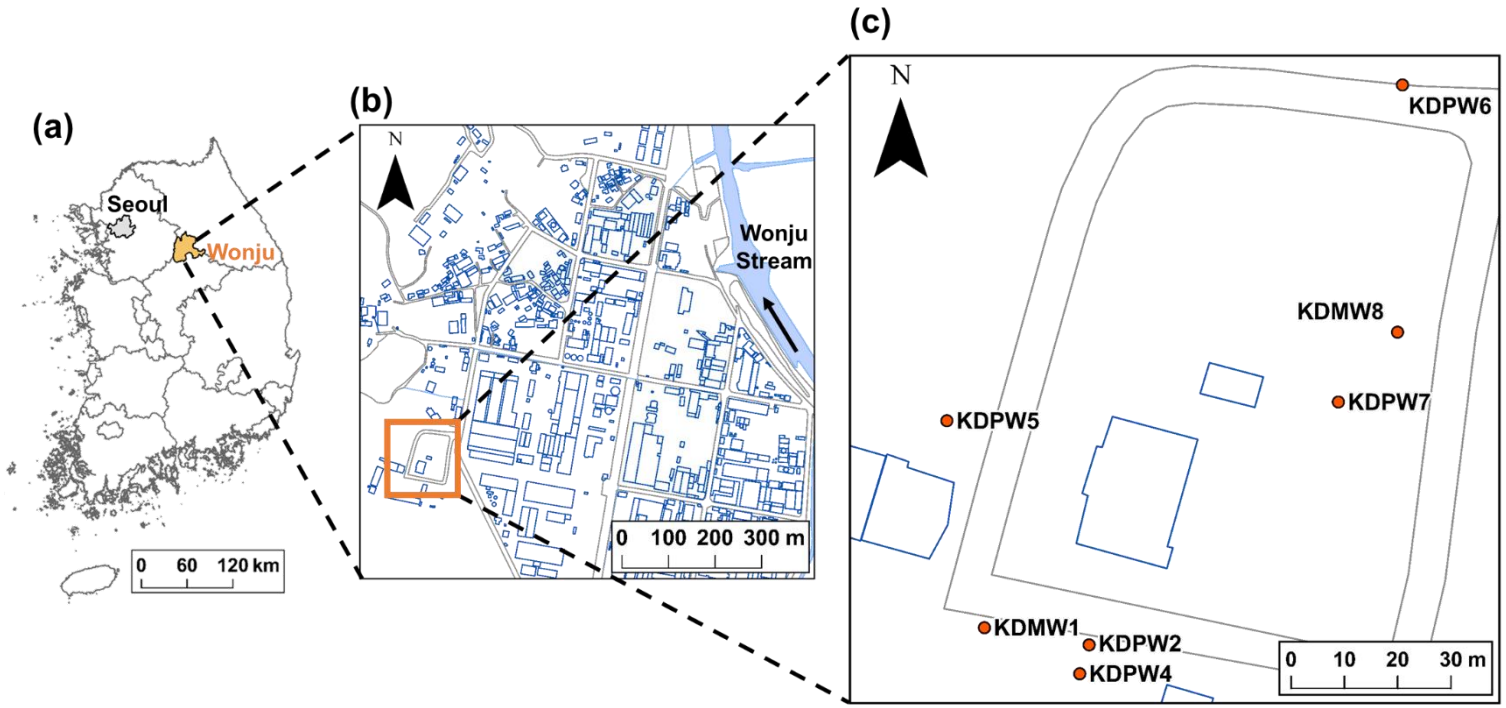

Figure 2-1 (a) Map of the Republic of Korea. (b) Map of Wonju with RAO marked in orange box. (c) Map with the wells used for groundwater sampling at RAO marked in orange dots.

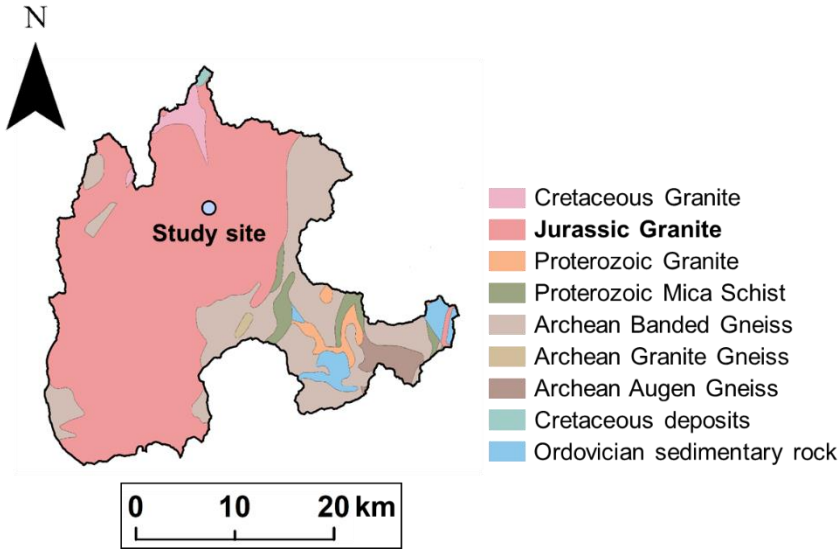

Figure 2-2 Geology of the Wonju. The test site locates at the Jurassic granite region.

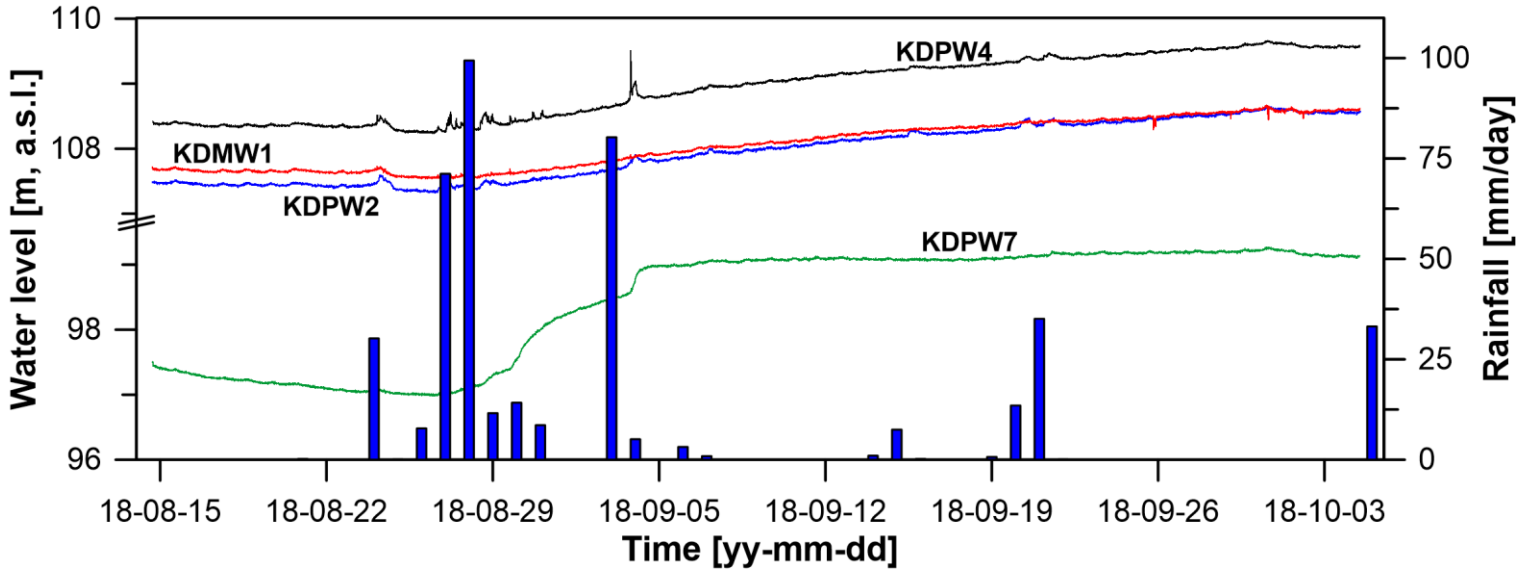

Figure 2-3 Water level fluctuation observed from monitoring wells KDPW2, 4, 7 and KDMW1 with daily rainfall rate from Wonju weather station operated by the Korea Meteorological Administration (KMA) (August 2018–October 2018).

3. METHODOLOGY

3.1 Sample collection and analytical techniques

Groundwater was sampled from well KDPW2, 4, 5, 6, 7, KDMW1, and 8 at WIC region for noble gas analysis (Figure 2-1) one time each in August and October 2018. These wells were selected because they are located in the area highly contaminated with TCE (Lee et al., 2015; Yang and Lee, 2012). Sampling dates are chosen by looking at the real-time groundwater level monitoring data at Woosan-dong, Wonju provided from Groundwater Information Management and Service Center (http://www.gims.go.kr). From the previous study by Yang and Lee (2012) and Yang et al. (2012), Wonju region was known to show TCE concentration relevant with seasonal hydrological variations. Therefore, August 14, 2018 and October 4, 2019 were chosen because they were two points during the test period with low and high groundwater levels.

Groundwater samples were pumped out from the well by submersible and controllable quantitative pump (MP1, Van Walt Ltd, England). Noble gas samples should be acquired without any contact with the atmosphere or other external sources to avoid possible pollution. Therefore, extra care should be followed during the sampling process. The sampling system was designed to make the water flow along with the polyethylene (PE) pipe and then to the flexible tubing connected to the copper tube which is fixed on

the steel rack with clamps at each end (Figure 3-1). Two sets of copper tubes on steel rack were set to obtain duplicate in case of a mistake during further procedures. After ensuring there were no air bubbles inside both PE pipe and flexible tubing, both valves were closed starting from the valve closer to the outlet. Finally, the clamps were tightened using the wrench. The copper tubes were then removed from the rack and it can preserve even the most vulnerable He content semi-permanently for future analysis (Burnard, 2013).

Copper tubes were then sent to the noble gas lab at the University of Utah, USA for further analysis (Aeschbach-Hertig and Solomon, 2013; Solomon et al., 2015). Only gas fraction in groundwater samples were extracted prior to the analysis. Then, the refined gas sample was loaded to the preparation line to be separated into each gas component (He, Ne, Ar, Kr, and Xe) according to their releasing temperature. Finally, the sample is sent to the mass spectrometer (RGA 300, Stanford Research Systems, United States) and the reproducibility of this method was within 1% for He and within 5% for the other noble gases (Manning et al., 2005; Solomon et al., 2010). Gas standards were measured to convert the output signal to concentration. Standards were analyzed every time after sample measurement to reflect the exact condition of the mass spectrometer which could be slightly different every day.

As for TCE analysis, groundwater samples were sampled in 40 ml amber glass vials with no headspace. All samples were sent to the laboratory at

Sangji University, Korea in a day and analyzed using the Varian Saturn 2100T gas chromatography/mass spectrometry.

O and H isotopes were measured at the Korea Basic Science Institute using the stable isotope ratio mass spectrometer. Results were converted to δ notation relative to Vienna Standard Mean Ocean Water (V-SMOW) with a precision lower than ±1 ‰ for both $\delta^{18}O$ and δD. Information about the devices used for groundwater analysis is listed in Table 3-1.

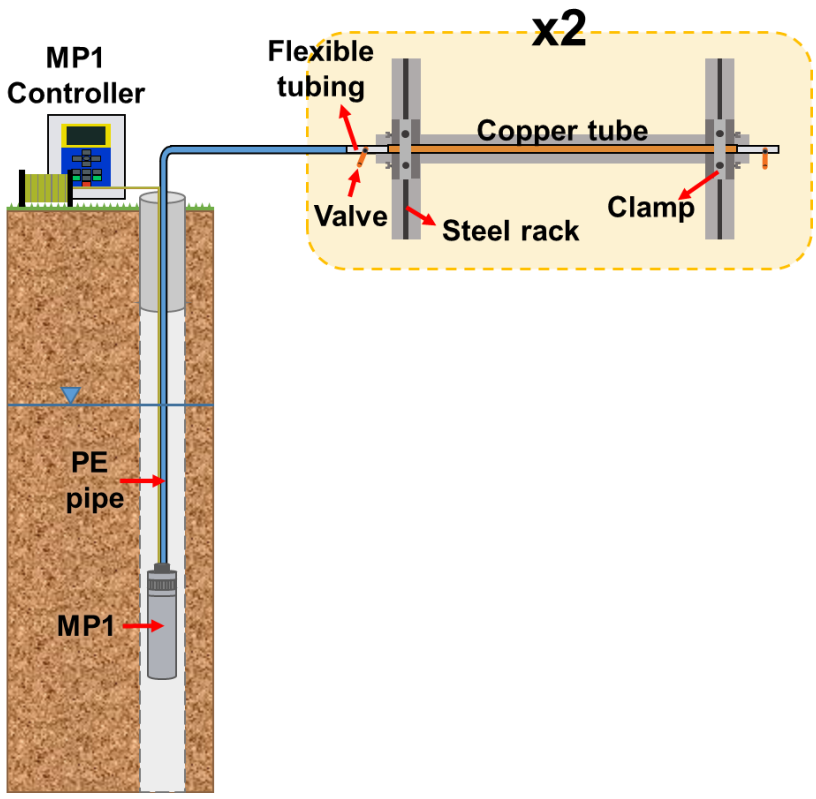

Figure 3-1 Groundwater sampling system using copper tube samplers for noble gas analysis.

Table 3-1 List of in-lab analyzed factors and used devices.

	Device	Precision
Noble gas	Quadrupole mass spec. (RGA 300, SRS, USA)	2% (for He)
		5% (for other components)
TCE	GC/MS (VARIAN Saturn 2100T, Agilent, USA)	-
O·H isotope	SIRMS (DELTA V, Thermo Fisher, USA)	±0.1‰ (for $\delta^{18}O$)
		±1 ‰ (for δD)

3.2 He source identification

Evolution of groundwater from their recharge conditions are often identified using He isotope evolution plot with excess air corrected ratio of ^{3}He and ^{4}He (Aeschbach-Hertig et al., 1998; Baskaran, 2011). This method is widely used in various sites around the world (Kaown et al., 2014; Koh et al., 2006; Kulongoski et al, 2008). The total He concentration in the sample is separated into equilibrated and exceeding concentrations using Noble90 for this plot (Aeschbach-Hertig et al., 1999). “Excess air” is the part of the gas that literally exceeds the equilibrium concentration and there are several excess air models to calculate noble gas concentration in groundwater.

First, the unfractionated air model assumes the complete dissolution of the captured air. Partial degassing (PD) model is the first degassing model with the concept that total gas concentration is affected by diffusion-controlled gas exchange across the water table after the initial complete dissolution of trapped air bubbles. Next is partial re-equilibration (PR) model, which resembles the PD model, except that here diffusive gas loss affects only the excess air portion. Light noble gases with higher diffusivities are preferentially lost, and the remaining excess of dissolved gases is enriched. Last is the closed-system equilibration (CE) model. The concept of this model assumes that trapped air bubbles do not completely dissolve but reach solubility equilibrium at a quasi-saturated zone due to

hydrostatic loading. The supersaturated water that is enriched relative to the air in heavier noble gases, reproducing the observed mass fractionation of the excess air.

Measured noble gas concentrations are then fitted with excess air models above via Noble90 to calculate equilibrium and excess concentration. The result with minimum χ^2 (chi-square) is chosen to plot ($^3He_{tot}$-$^3He_{exc}$)/($^4He_{tot}$-$^4He_{exc}$) to $^4He_{eq}$/($^4He_{tot}$-$^4He_{exc}$) graph for He source identification. He_{tot} stands for total He concentration in the sample, and He_{exc} stands for excess air component of He. The X and Y-axis of the plot are excess air corrected ^{4}He and excess air corrected ratio of ^{3}He and ^{4}He. He concentration in the groundwater sample is consisted of air equilibrated He (He_{eq}), excess air derived He (He_{exc}), terrigenic He which is originated mainly from solid earth including the rock medium within where the groundwater is located for both of the He components and additionally, the radioactive decay of tritium in the water is another source in case of ^{3}He (Aeschbach-Hertig et al., 1998). Therefore, by calculating the excess air derived He using Noble90, it is able to verify the effect of non-atmospheric sources such as terrigenic, radiogenic and tritiogenic ^{3}He.

This plot clearly shows the share of each component, making it easier to determine the dominant process that affected the groundwater systems from recharge conditions. Notable references to add in this plot are the evolutionary trajectory (Line that crosses Air Saturated Water (ASW) with y-axis intercept as $0.02R_A$) representing the addition of radiogenic He to

ASW and addition of tritiogenic ^{3}He ($^{3}He/^{4}He = \infty$) (Baskaran, 2011). If sample plots follow the reference line, this shows the effect of radiogenic crustal ^{4}He or addition of tritiogenic ^{3}He.

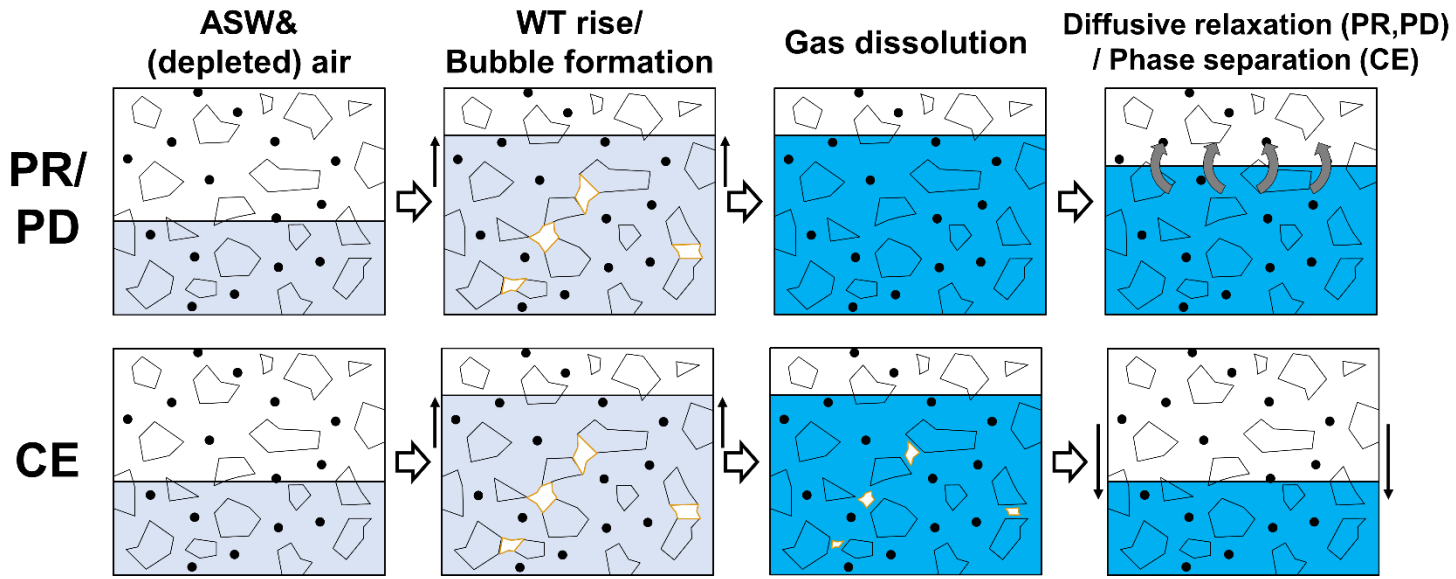

Figure 3-2 Schematic illustration of the processes assumed in the various excess air models used in Noble90 (Aeschbach-Hertig et al., 1999). With the best-fit model, noble gas components are divided into He_{eq}, and He_{exc} (PR: Partial Re-equilibration, PD: Partial Degassing, CE: Closed-system Equilibration) (Burnard, 2013).

3.3 Partitioning behavior of noble gas

Noble gases show interactions between different fluid phases through its partitioned concentration (Ballentine et al., 2002). Whether the reacting system is open or closed plays an important role in noble gas partitioning. In a closed system where the amount of each phase is limited, the noble gas concentration follows batch fractionation. In an open system where the reacting phase is continuously removed and replenished, the Rayleigh equation governs the process.

In a closed system, when the TCE fraction in the water with noble gas decreases, the least soluble noble gases will tend to be enriched in the TCE. During the fractionation, the limit of the saturation is controlled by the relative solubility of each noble gas. Henry's Law explains the fractionation of noble gas between the TCE and water with which it is in equilibrium. With the assumption of ideal gas behavior, Henry's law can be rewritten to relate the concentration in the TCE (C_{TCE}^{i}) and water phase (C_{l}^{i}), where K_{i}^{d} stands for Henry's constant (Eq. 1).

$$C_{TCE}^{i} = K_{i}^{d} C_{l}^{i} \qquad \text{(Eq. 1)}$$

The equilibrium concentrations of each phase also have a relationship with the TCE, water volume ratio (V_l/V_{TCE}), related by Eq. 2, where $[i]_{TCE}$ is the number of moles in the TCE phase and $[i]_{tot}$ is the total number of moles.

$$[i]_{TCE} = [i]_{tot}(V_l/V_{TCE}K_i^d + 1)^{-1} \quad \text{(Eq. 2)}$$

By using Henry's constant with units of atm, Henry's law is organized into molality units and expressed as Eq. 3.

$$[\mathrm{i}]_{\mathrm{TCE}} = [i]_{tot}\left[\frac{22400\mathrm{T}\rho_l V_l}{1000 \times 273\frac{\gamma_i}{\phi_i}K_i^m V_{TCE}} + 1\right]^{-1} \quad \text{(Eq. 3)}$$

In Eq. 3, ρ_l is the density of the water [g/cm^3], T stands for temperature [K] and $V_{l,TCE}$ is volume of water (l), or TCE in cm^3. The calculated noble gas concentrations are expressed using F notation (Eq. 4).

$$F(i) = ([i]/[Ar])_{sample}/([i]/[Ar])_{ASW} \quad \text{(Eq. 4)}$$

In equation 4, i stands for the noble gas component, [] stands for concentration of each component and ASW is an acronym for Air Saturated Water which is used as an end-member in this study. ASW of 13°C which was one of the sample's actual temperatures was used in this study. Table 3-2 shows concentrations of each noble gas components at 13°C ASW. F is an Ar normalized ratio of noble gas distribution in the sample, in this case, TCE and water. F value is often used to explain the partitioning behavior of noble gas in the oil and natural gas fields. Among 5 components, Ar is used because of the mass-dependent solubility change of noble gases. Figure 3-3 shows the solubility ratio of noble gas components in 50°C gas, oil, and water. Ar has a median value of solubility to heavy oil among noble gas

components, and by normalizing solubility with Ar, heavier components which have higher solubility to heavy oil will show positive change when partitioned to more soluble substance and lighter components such as He and Ne will show negative change which will clearly show the effect of partitioning.

In the open system, the continuous reaction is expressed in exponential variation in the equation.

$$\left(\frac{[\mathrm{i}]}{[\mathrm{Ar}]}\right)_{\mathrm{sample}} = \left(\frac{[\mathrm{i}]}{[\mathrm{Ar}]}\right)_{\mathrm{ASW}} P^{(\alpha-1)} \qquad \text{(Eq. 5)}$$

$$\alpha = (\mathrm{K_i^{water}K_{Ar}^{TCE}})/(\mathrm{K_i^{TCE}K_{Ar}^{water}}) \qquad \text{(Eq. 6)}$$

In Eq. 5, P is the fraction of Ar remaining in the water phase, ([i]/[Ar]) is the i/Ar ratio in each phase and α is the fractionation coefficient. In this study, the Rayleigh fractionation coefficient used to determine the magnitude of fractionation in a water phase that has interacted with TCE is given as Eq. 6.

In case of noble gas solubility to TCE, only the constants for He and Ne at 20°C are studied (Divine et al., 2003). In this paper, He is excluded as a partitioning tracer due to dominant radiogenic sources. With radiogenic input being the major mechanism affecting He concentration, it is relatively hard to distinguish the effect of partitioning. Moreover, the constants from Divine et al. (2003) were acquired at temperature condition of 20°C, while

the groundwater samples from the on-site experiment of this study were 13–15.2°C. Therefore, solubility constant at 13°C for heavy oil which can be representative of NAPL species is used instead (Kharaka and Specht, 1988).

To calculate the solubility of noble gas to 13°C heavy oil, a linear relationship between log K* and the temperature was used (Eq. 7).

$$\log K^* = a + bt \qquad \text{(Eq. 7)}$$

K* is the solubility constant expressed in atm · kg/mol, t is the temperature in °C. Constants a and b for each noble gas components are listed in Table 3-3. To convert K* into K_i^{water}/K_i^{TCE} the ratio which is required at Eq. 2, Henry's constant for noble gas components in water solution should be divided. Henry's constant for noble gas components in water solution can be calculated in various temperatures by using Eq. 8.

$$k_H(T) = k_H^{\circ} \exp\left(\frac{d(\ln k_H)}{d\left(\frac{1}{T}\right)}\left(\frac{1}{T} - \frac{1}{298.15K}\right)\right) \qquad \text{(Eq. 8)}$$

$k_H(T)$ is the Henry's constant for noble gas components in water solution [mol/kg·bar], $k°_H(T)$ is the Henry's law constant for solubility in water at 298.15 K [mol/kg·bar], and $d(\ln(k_H))/d(1/T)$ stands for temperature dependence constant [K] listed at Table 3-4. The solubility ratio of each noble gas components at 13°C to heavy oil was obtained using the equations above as listed in Table 3-5.

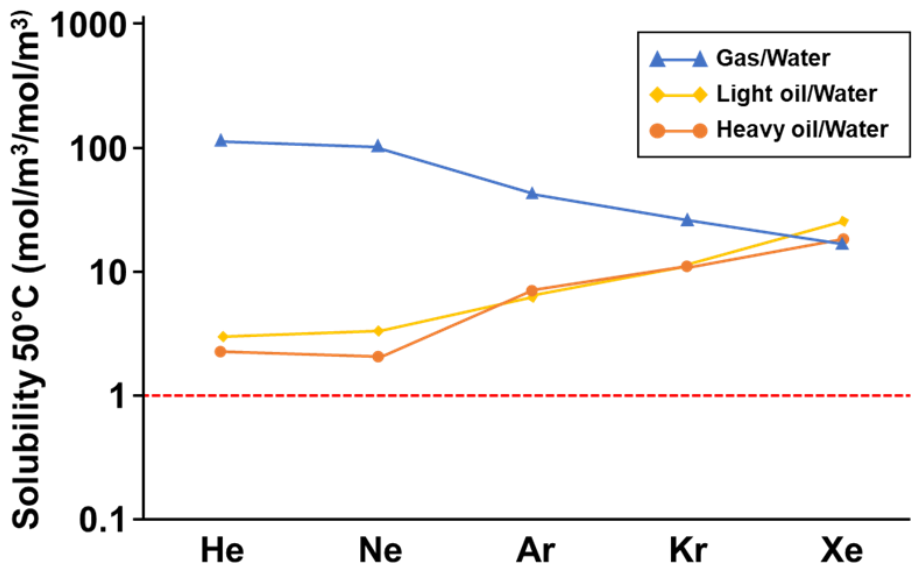

Figure 3-3 Solubility ratio of noble gas components in 50°C gas, oil and water (Burnard, 2013).

Table 3-2 Noble gas concentration of 13°C ASW.

T= 13°C (ASW)	**Ne**	**Ar**	**Xe**
Concentration [cm^3STP/g]	1.96×10^{-7}	3.61×10^{-4}	8.37×10^{-8}

Table 3-3 Values of coefficients a and b relating log K* values to temperature

	a	**b**
He	3.250	-0.0054
Ne	3.322	-0.0063
Ar	2.121	-0.0003
Kr	1.607	0.0019
Xe	1.096	0.0035

Table 3-4 Temperature dependence constant for each noble gas component

	He	**Ne**	**Ar**	**Kr**	**Xe**
$d(\ln(k_H))/d(1/T)$	360	530	1100	1500	1900

Table 3-5 Partitioning coefficient of 13°C heavy oil and water.

T= 13°C	Ne	Ar	Xe
Partitioning coefficient (oil/water)	1.171	4.612	12.684

4. RESULTS AND DISCUSSION

4.1 He distribution of the study site

Since noble gases are inert, there are very limited sources that bring changes to noble gas concentration in groundwater. Figure 4-1 shows various influences affecting the noble gas concentration in groundwater. Among these processes, excess air injection due to water table fluctuation, radiogenic influences and partitioning to TCE are thought to affect noble gas concentrations the most in the study site. To clearly verify the influence of TCE contamination, other factors are considered first by looking at the background hydrogeology of the study site using He isotope prior to partitioning analysis.

^{4}He is a well-known parameter showing the influence of radiogenic source among noble gas isotopes. On the excess air corrected (He_{exc}) plot of ^{3}He and ^{4}He (Figure 4-2), all samples obtained from the study area follow the radiogenic trajectory line other than routes showing the influence of terrigenic or tritiogenic sources. The study site is located in the region with Jurassic granite as a bedrock. Granite is well known to have various radionuclides such as U and Th, which produce the ^{4}He by α-decay product. Also, the granite located at the study site is highly fractured (Baek and Lee, 2011; Yu et al., 2006), being a great pathway for radiogenic ^{4}He to move along and be collected (Torgersen and O'Donnell, 1991). Therefore,

samples from the study site show a clear pattern of He distribution influenced by radiogenic sources (Heaton, 1984; Kaown et al., 2014).

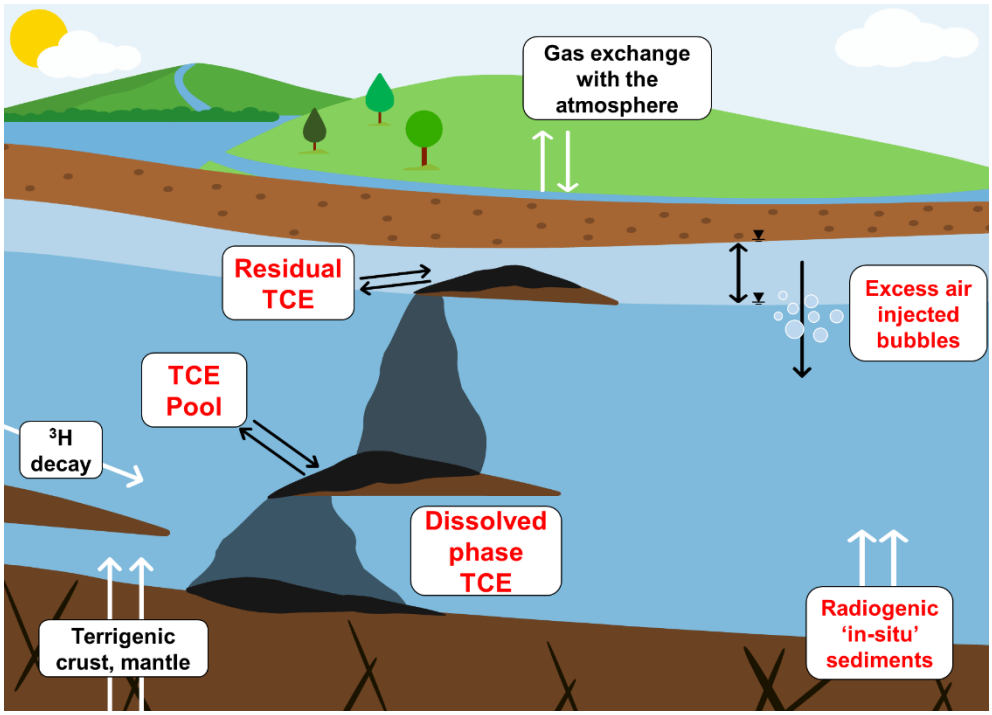

Figure 4-1 Schematic diagram of various influences including TCE contamination affecting noble gas concentrations. Red colored texts are possible dominant processes affecting noble gas distribution at Wonju.

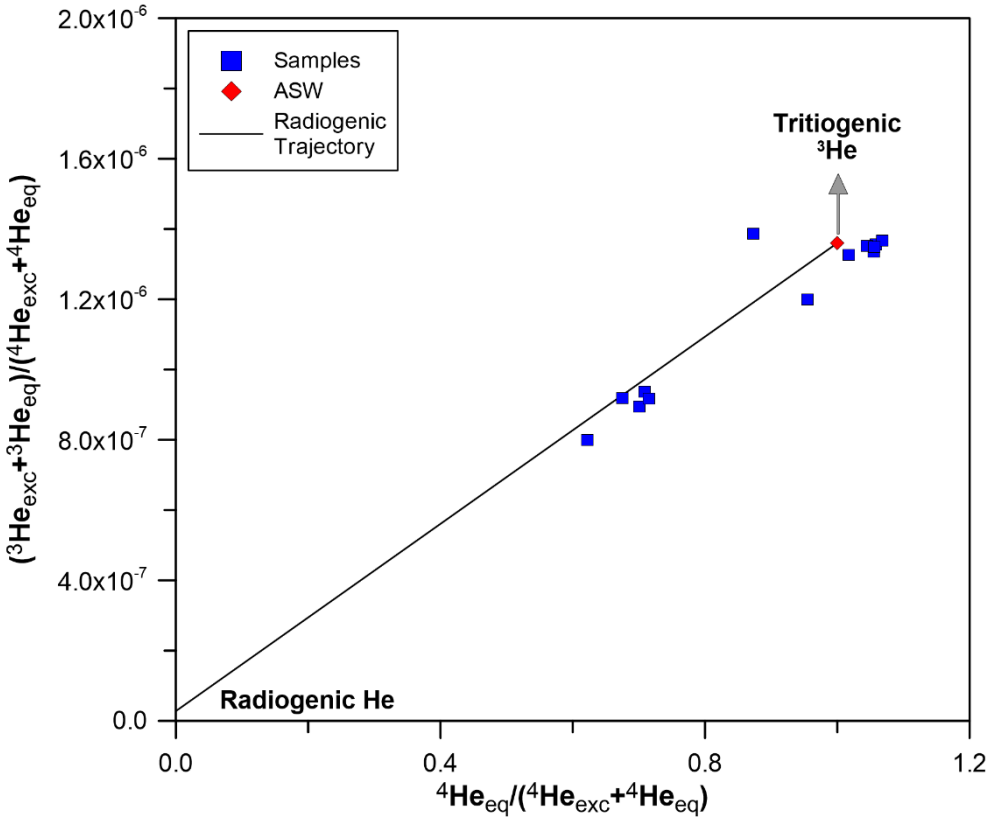

Figure 4-2 Excess air corrected ratio of ^{3}He and ^{4}He for source identification of groundwater samples. Gray arrow show pattern for and tritiogenic sources. Solid line is a trajectory line for groundwater influenced by radiogenic source.

4.2 Quantifying and allocating residual TCE source using noble gas

Noble gas concentrations were processed with the equations above prior to partition analysis and converted into F notation (Table 4-1). F factors for all noble gas components were first compared with Noble90 calculated concentrations of ASW (Figure 4-3). ASW samples were calculated in total 4 conditions, for two temperature 13 and 15.2°C which are highest and lowest groundwater temperatures during the sampling period, and for two excess air conditions, 0 and 45 Ne% which are known to be the typical excess air range in nature (Gilfillan et al., 2008). In Figure 4-3, several noble gas components show clear variation exceeding the calculated natural range. Therefore, it is appropriate to say that there is an extra factor influencing the groundwater at WIC.

F factors of the samples are plotted on F_{Ne}, F_{Xe} graph with the calculated ideal partition lines of Rayleigh partitioning representing open system, and Batch equilibrium representing closed system in Figure 4-4. Partitioning lines in both open and closed systems are drawn on the graph. The numbers along the lines from 0.01 to 0.07 are TCE/water ratios of the point. From the distance with ideal lines, samples could be divided into two groups. Samples that are close with the fractionation lines are from well KDPW 2, 4, 7 and KDMW 1, 8 in ‘Group 1’ and match the ones with TCE concentration over 150 μg/L in Table 4-2. Therefore, the source of TCE

contamination will be near the wells in the ‘Group 1’. Their location on the plot also implies TCE volume in the system. In this case, total TCE including TCE pools that are not properly dissolved will be 0.03–0.05 relative with the water volume underground when calculated with Henry’s constant of heavy oil.

Points in the plot showing least accordance with either of the fractionation lines are ‘Group 2’ samples showing that they are influenced by other mechanisms rather than partitioning to TCE. By comparing with excess air influenced samples in cross symbols, the ‘Group 2’ samples are expected to be first influenced by partitioning with a small amount of TCE and later mostly diluted by the addition of excess air.

4.3 Effect of water level fluctuation to noble gas partitioning

In Wonju, groundwater level rises from August to October (Table 4-2). In KDPW 6, where the water level rise is the highest, the level difference between the two seasons is about 3.99 m by using manually measured water level. Rainfall is concentrated in summer and early fall throughout the year at the study site. Therefore, this water level rise is thought to be due to the infiltration of rainwater. According to the O-H isotope data, groundwater in both sampling periods tend to follow the Local Meteoric Water Line (LMWL) for wet season from Lee (1999), suggesting that most of the recharge took place during the wet season when intensive precipitation occurred (Figure 4-5) (Kaown et al., 2014).

Despite the introduction of uncontaminated rainwater, every test wells show an increase in TCE concentration in October (Table 4-2). This increase is relevant to the previous study by Yang and Lee. (2012) and Yang et al. (2012) that groundwater in the main source zone can be affected by residual TCE in the lower unsaturated zone when the groundwater level rises.

This seasonal variation is also found in the noble gas analysis (Figure 4-6). Samples from only the ‘Group 1’ zone are plotted along with ideal batch equilibrium and Rayleigh fractionation line again and divided into two groups according to their sampling date (Table 4-1). From August 2018 to October 2018, samples shift from right to left in the figure, getting closer to

the Rayleigh fractionation line. In August, noble gas was relatively in equilibrium between groundwater and TCE. However, as the water table rises, noble gas became open with residual TCE, which is a receiving fluid in the water-TCE system.

Table 4-1 F factors of noble gas samples from WIC.

	Name	F_{Ne}	F_{Xe}
Group 1	KDPW4 (Aug)	1.149	0.813
	KDPW2 (Aug)	1.137	0.846
	KDMW1 (Aug)	1.155	0.831
	KDPW7 (Aug)	1.109	0.883
	KDMW8 (Aug)	1.141	0.853
	KDPW4 (Oct)	1.088	0.830
	KDMW1 (Oct)	1.108	0.801
	KDPW7 (Oct)	1.113	0.845
	KDPW8 (Oct)	1.124	0.870
Group 2	KDPW5 (Aug)	1.234	0.773
	KDPW6 (Aug)	1.329	0.838
	KDPW5 (Oct)	1.047	0.516
	KDPW6 (Oct)	1.266	0.877

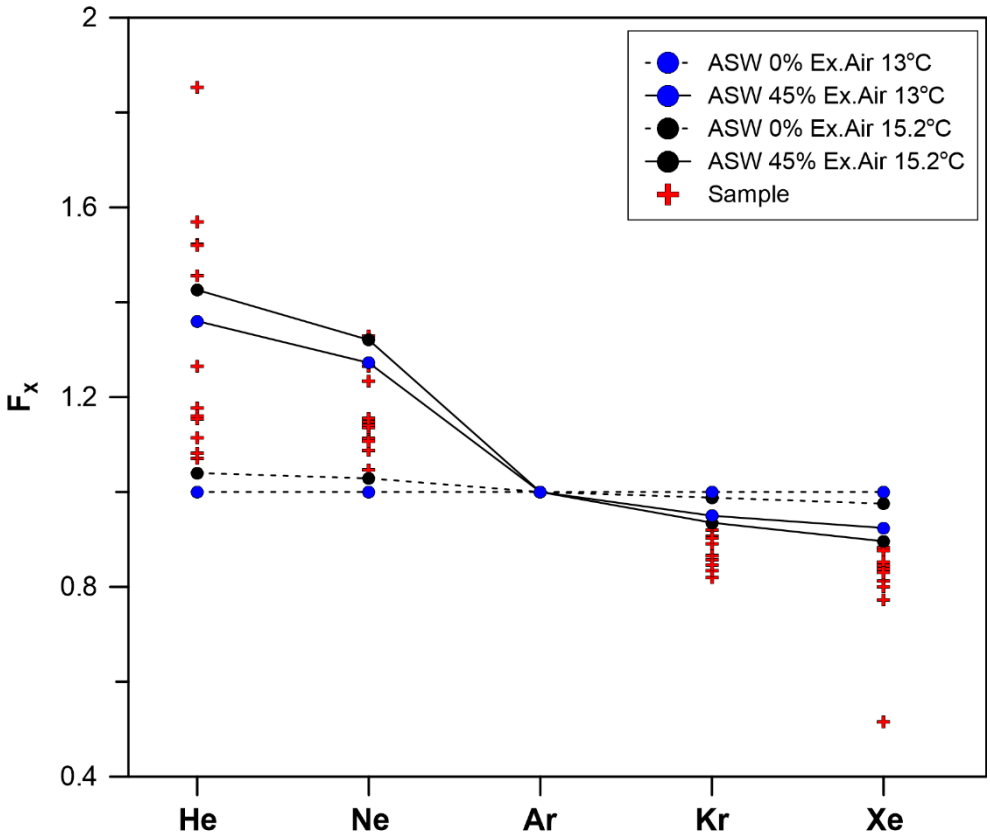

Figure 4-3 Comparing sample plots and partitioning range of all noble gas components in typical excess air range (–45%) during natural variation.

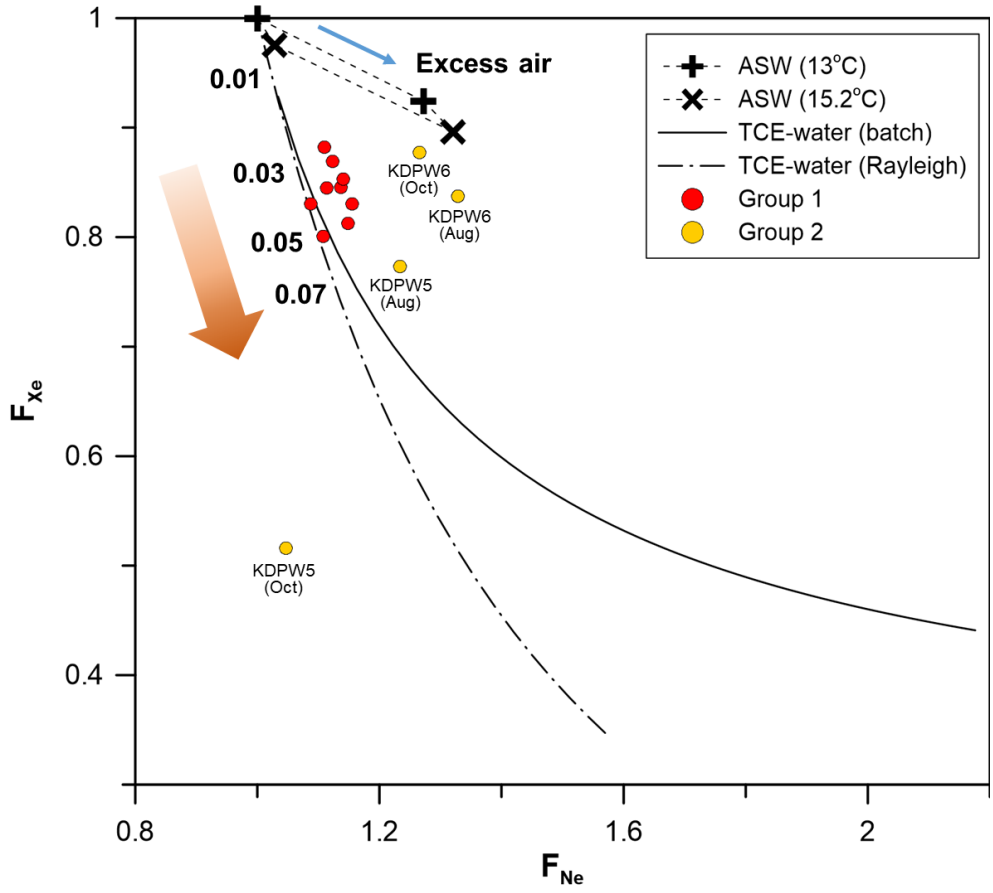

Figure 4-4 Noble gas fractionation and its relationship with TCE/water ratio of WIC samples. Samples are acquired at two different sampling dates, August and October 2018. Numbers along the TCE-water fractionation line indicate TCE/water ratio in the system. Along the blue arrow, excess air ratio increases up to 45% which is typical excess air range in natural situations.

Table 4-2 Water table fluctuation and TCE concentration change between August and October 2018.

	Water table fluctuation (Oct-Aug) [m]	**TCE (Aug) [μg/L]**	**TCE (Oct) [μg/L]**	**TCE concentration change rate [%]**
KDPW4	1.15	1223	1376	12.5
KDPW2	1.08	994	-	-
KDMW1	1.14	517	578	11.7
KDMW8	2.52	171	179	4.6
KDPW7	2.99	165	196	18.9
KDPW6	3.99	44	66	49.2
KDPW5	0.17	40	48	21.3

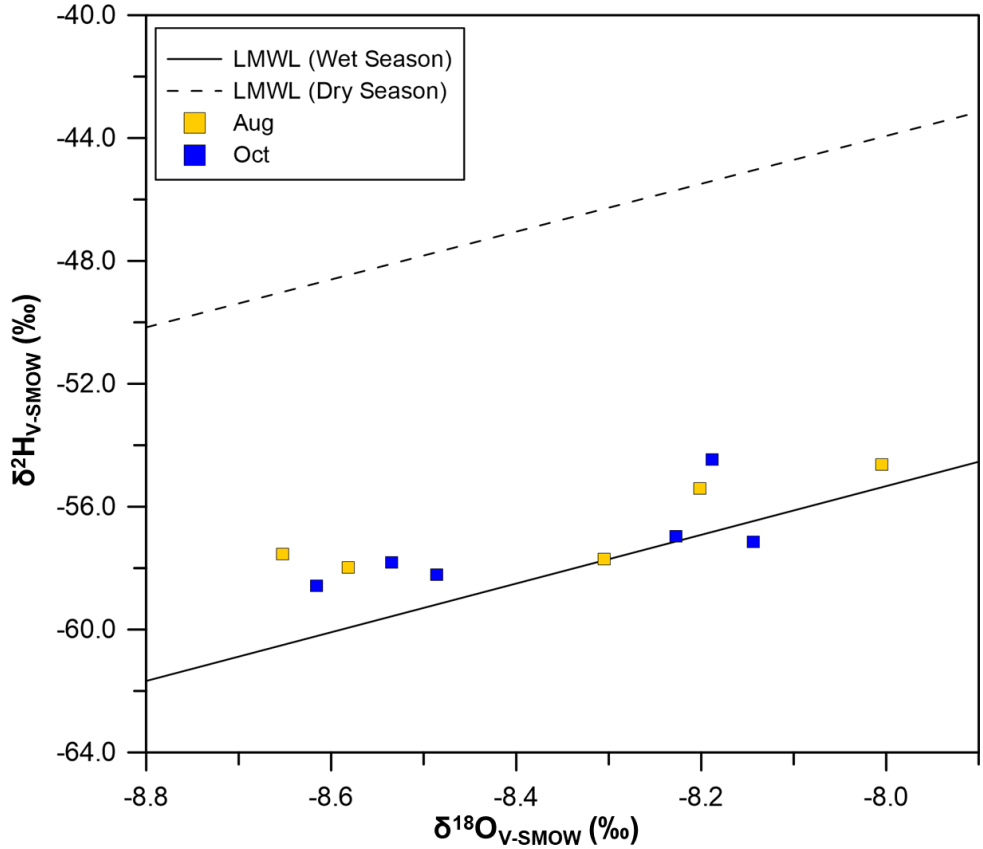

Figure 4-5 O and H isotopic compositions in groundwater samples with Local Meteoric Water Line (LMWL) in wet and dry seasons of Korea (Lee, 1999).

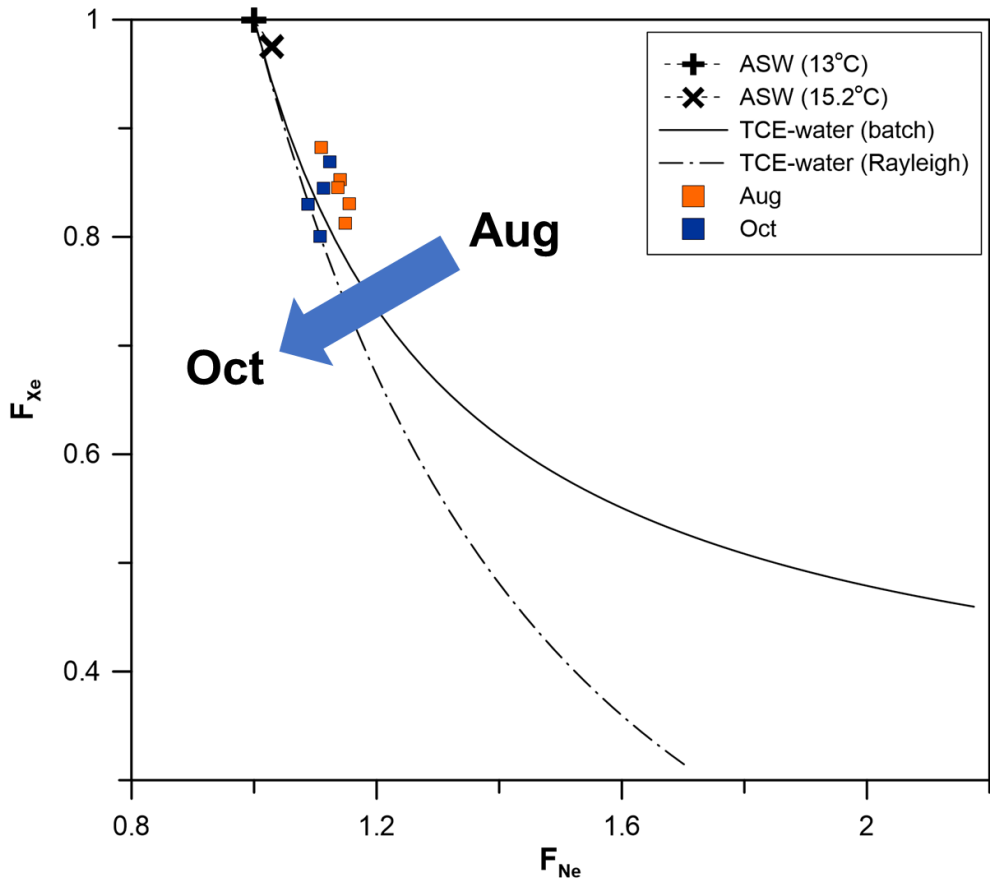

Figure 4-6 Noble gas fractionation and its relationship with seasonal variation of WIC samples. Blue arrow shows shift of samples from August to October 2018.

5. CONCLUSION

Noble gas concentrations and its partitioning nature were used to calculate the total TCE/water ratio in the field-scale groundwater system and allocate the TCE source. He source distribution analysis was done prior to the discussion about TCE contamination and showed that the groundwater of the study site clearly shows the effect of radiogenic sources. With further study on partitioning behavior of noble gas to TCE based on Rayleigh fractionation and batch equilibrium scenarios, TCE/water ratio of the test site was calculated to be 0.03–0.05 and the main source area was found to be near the wells KDPW2, 4, 7, KDMW1, and 8. Moreover, it was found that noble gases can reflect the seasonal variations caused by water table fluctuation during the test period and TCE concentration increase by comparing it with two partitioning scenarios along with isotope compositions of O and H.

In this study, it was found that noble gas is a good tracer not only in the lab-scale experiment from the previous study but also in field-scale that reflects the seasonal variations derived from water table fluctuation and has implication in understanding the spatial distribution of TCE with approximate ratio of TCE and groundwater existing at the test site. Therefore, with more effort in measuring the solubility of all noble gas components to TCE in various temperature conditions, applying noble gas partitioning is suggested to be a promising method in the field-scale

characterization of the TCE contaminated site.

6. REFERENCES

Aeschbach-Hertig, W., Schlosser, P., Stute, M., Simpson, H. J., Ludin, A., & Clark, J. F., 1998. A $^{3}H/^{3}He$ study of ground water flow in a fractured bedrock aquifer. Groundwater, 36(4), 661-670. https://doi.org/10.1111/j.1745-6584.1998.tb02841.x

Aeschbach-Hertig, W., Peeters, F., Beyerle, U., & Kipfer, R., 1999. Interpretation of dissolved atmospheric noble gases in natural waters. Water Resources Research, 35(9), 2779-2792. https://doi.org/10.1029/1999WR900130

Aeschbach-Hertig, W., & Solomon, D. K., 2013. Noble gas thermometry in groundwater hydrology, in: Burnard, P. (Eds.), The Noble Gases as Geochemical Tracers, Springer, New York, pp. 81–122.

Baek, W., & Lee, J. Y., 2011. Source apportionment of trichloroethylene in groundwater of the industrial complex in Wonju, Korea: a 15-year dispute and perspective. Water and Environment Journal, 25(3), 336-344. https://doi.org/10.1111/j.1747-6593.2010.00226.x

Ballentine, C. J., & Burnard, P. G., 2002. Production, release and transport of noble gases in the continental crust. Reviews in Mineralogy and Geochemistry, 47(1), 481–538. https://doi.org/10.2138/rmg.2002.47.12

Ballentine, C. J., Burgess, R., & Marty, B., 2002. Tracing fluid origin, transport and interaction in the crust. Reviews in Mineralogy and Geochemistry, 47(1), 539–614. https://doi.org/10.2138/rmg.2002.47.13

Barry, P. H., Lawson, M., Meurer, W. P., Danabalan, D., Byrne, D. J., Mabry, J. C., & Ballentine, C. J., 2017. Determining fluid migration and isolation times in

multiphase crustal domains using noble gases. Geology, 45(9), 775–778. https://doi.org/10.1130/G38900.1

Baskaran, M. (Eds.), 2011. Handbook of environmental isotope geochemistry. Springer Science & Business Media.

Burnard, P., 2013. Advances in Isotope Geochemistry, Springer.

Chiu, W. A., Jinot, J., Scott, C. S., Makris, S. L., Cooper, G. S., Dzubow, R. C., Bale, A. S., Evans, M. V., Guyton, K. Z., Keshava, N., Lipscomb, J. C., Barone Jr, S., Fox, J. F., Gwinn, M. R., Schaum, J., & Caldwell, J. C., 2012. Human health effects of trichloroethylene: key findings and scientific issues. Environmental Health Perspectives, 121(3), 303–311. https://doi.org/10.1289/ehp.1205879

Davis, B. M., Istok, J. D., & Semprini, L., 2002. Push–pull partitioning tracer tests using radon-222 to quantify non-aqueous phase liquid contamination. Journal of Contaminant Hydrology, 58(1–2), 129–146. https://doi.org/10.1016/S0169-7722(02)00010-4

Divine, C. E., Sanford, W. E., & McCray, J. E., 2003. Helium and neon groundwater tracers to measure residual DNAPL. Vadose Zone Journal, 2(3), 382-388. https://doi.org/10.2136/vzj2003.3820

Gilfillan, S. M., Ballentine, C. J., Holland, G., Blagburn, D., Lollar, B. S., Stevens, S., & Cassidy, M., 2008. The noble gas geochemistry of natural CO_2 gas reservoirs from the Colorado Plateau and Rocky Mountain provinces, USA. Geochimica et Cosmochimica Acta, 72(4), 1174–1198. https://doi.org/10.1016/j.gca.2007.10.009

Gilfillan, S. M., Sherk, G. W., Poreda, R. J., & Haszeldine, R. S., 2017. Using noble gas fingerprints at the Kerr Farm to assess CO_2 leakage allegations linked to the Weyburn–Midale CO_2 monitoring and storage project. International Journal of Greenhouse Gas Control, 63, 215–225. https://doi.org/10.1016/j.ijggc.2017.05.015

Heaton, T. H. E., 1984. Rates and sources of ^{4}He accumulation in groundwater. Hydrological Sciences Journal, 29(1), 29–47. https://doi.org/10.1080/02626668409490920

Istok, J. D., Field, J. A., Schroth, M. H., Davis, B. M., & Dwarakanath, V., 2002. Single-well "push–pull" partitioning tracer test for NAPL detection in the subsurface. Environmental Science & Technology, 36(12), 2708–2716. https://doi.org/10.1021/es015624z

Kao, C. M., & Lei, S. E., 2000. Using a peat biobarrier to remediate PCE/TCE contaminated aquifers. Water Research, 34(3), 835–845. https://doi.org/10.1016/S0043-1354(99)00213-4

Kaown, D., Koh, D. C., Solomon, D. K., Yoon, Y. Y., Yang, J., & Lee, K. K., 2014. Delineation of recharge patterns and contaminant transport using ^{3}H–^{3}He in a shallow aquifer contaminated by chlorinated solvents in South Korea. Hydrogeology Journal, 22(5), 1041–1054.

Kharaka, Y. K., & Specht, D. J., 1988. The solubility of noble gases in crude oil at 25–100°C. Applied Geochemistry, 3(2), 137–144. https://doi.org/10.1016/0883-2927(88)90001-7

Koh, D. C., Plummer, L. N., Solomon, D. K., Busenberg, E., Kim, Y. J., & Chang, H. W., 2006. Application of environmental tracers to mixing, evolution, and nitrate

contamination of ground water in Jeju Island, Korea. Journal of Hydrology, 327(1-2), 258–275. https://doi.org/10.1016/j.jhydrol.2005.11.021

Kulongoski, J. T., Hilton, D. R., Cresswell, R. G., Hostetler, S., & Jacobson, G., 2008. Helium-4 characteristics of groundwaters from Central Australia: Comparative chronology with chlorine-36 and carbon-14 dating techniques. Journal of Hydrology, 348(1-2), 176–194. https://doi.org/10.1016/j.jhydrol.2007.09.048

Lee, K. S., 1999. Oxygen and hydrogen isotopic composition of precipitation and river waters in South Korea. Journal of the Geological Society of Korea, 35, 73–84.

Lee, S. S., Kaown, D., & Lee, K. K., 2015. Evaluation of the fate and transport of chlorinated ethenes in a complex groundwater system discharging to a stream in Wonju, Korea. Journal of Contaminant Hydrology, 182, 231-243. https://doi.org/10.1016/j.jconhyd.2015.09.005

Monosson, E., 2008. TCE contamination of groundwater. http://www.eoearth.org/ (accessed 05 December 2019).

Pinti, D. L., & Marty, B., 1995. Noble gases in crude oils from the Paris Basin, France: Implications for the origin of fluids and constraints on oil-water-gas interactions. Geochimica et Cosmochimica Acta, 59(16), 3389–3404. https://doi.org/10.1016/0016-7037(95)00213-J

Russell, H. H., Matthews, J. E., & Guy, W. S., 1992. TCE removal from contaminated soil and groundwater, in: Boulding, J. R. (Eds.), EPA Environmental Engineering Sourcebook, Routledge, pp. 87–100.

Solomon, D. K., Genereux, D. P., Plummer, L. N., & Busenberg, E., 2010. Testing mixing models of old and young groundwater in a tropical lowland rain forest with environmental tracers. Water Resources Research, 46(4). https://doi.org/10.1029/2009WR008341

Solomon, D. K., Gilmore, T. E., Solder, J. E., Kimball, B., & Genereux, D. P., 2015. Evaluating an unconfined aquifer by analysis of age-dating tracers in stream water. Water Resources Research, 51(11), 8883–8899. https://doi.org/10.1002/2015W R017602

Torgersen, T., & O'Donnell, J., 1991. The degassing flux from the solid earth: release by fracturing. Geophysical Research Letters, 18(5), 951-954. https://doi.org/10.1029/91GL00915

Yang, J. H., Jun, S. C., Kwon, H. P., & Lee, K. K., 2014. Tracing of residual multiple DNAPL sources in the subsurface using ^{222}Rn as a natural tracer at an industrial complex in Wonju, Korea. Environmental Earth Sciences, 71(1), 407–417. https://doi.org/10.1007/s12665-013-2448-2

Yang, J. H., & Lee, K. K., 2012. Locating plume sources of multiple chlorinated contaminants in groundwater by analyzing seasonal hydrological responses in an industrial complex, Wonju, Korea. Geosciences Journal, 16(3), 301–311. https://doi.org/10.1007/s12303-012-0028-1

Yang, J. H., Lee, K. K., & Clement, T. P., 2012. Impact of seasonal variations in hydrological stresses and spatial variations in geologic conditions on a TCE plume at an industrial complex in Wonju, Korea. Hydrological Processes, 26(3), 317–325. https://doi.org/10.1002/hyp.8236

Young, C. M., Jackson, R. E., Jin, M., Londergan, J. T., Mariner, P. E., Pope, G. A., Anderson., F. J., & Houk, T., 1999. Characterization of a TCE DNAPL zone in alluvium by partitioning tracers. Groundwater Monitoring & Remediation, 19(1), 84–94. https://doi.org/10.1111/j.1745-6592.1999.tb00190.x

Yu, S. Y., Chae, G. T., Jeon, K. H., Jeong, J. S., & Park, J. G., 2006. Trichloroethylene contamination in fractured bedrock aquifer in Wonju, South Korea. Bulletin of Environmental Contamination & Toxicology, 76(2). https://doi.org/10.1007/s00128-006-0927-9

Zaikowski, A., & Spangler, R. R., 1990. Noble gas and methane partitioning from ground water: An aid to natural gas exploration and reservoir evaluation. Geology, 18(1), 72–74. https://doi.org/10.1130/0091-7613(1990)018<0072:NGAMPF>2.3.CO;2

국문 초록

분배성 추적자 중에서도 비활성기체는 특히 생물화학적 반응에 참여하지 않아 물리적 기작을 더 명확히 확인할 수 있다는 장점이 있다. 비활성기체는 이러한 성질 때문에 석유나 천연 가스 저류층에서 매장량 평가를 위해 활용되어 왔으며, 대표적인 지하수 오염 물질로 인체의 많은 부분에 악영향을 주는 것으로 알려진 TCE 오염을 확인하는데 활용될 수 있음이 실내 실험 규모에서 증명된 바 있다. 본 연구에서는 이를 확장시켜 비활성기체의 분배성 추적자로서의 성질을 현장 규모의 TCE 오염 지하수 상황에 적용해보고자 하였다.

연구 지역은 국내에서 TCE 오염 지역으로 많은 연구가 이루어진 강원도 원주의 우산 공단 지역이다. 우산 공단 내에서 지하수 시료를 채취하여 시료 내 비활성기체 분포가 TCE 오염으로 인해 예상되는 분배 작용의 결과와 잘 일치하는지 확인하고자 하였다. 분석 결과는 두가지 분배 기작 모델인 Rayleigh fractionation, Batch equilibrium과 비교하여 해석하였다. 결과적으로 실제 TCE 오염 지역에서 비활성기체를 활용하여 TCE 오염의 분포와 그 존재 비율을 알 수 있었고, 수위 변동에 따른 잔류 TCE의 유입으로 인한 변화 역시 확인할 수 있었다.

본 연구를 통해 비활성기체가 다양한 상이 존재하는 시스템에서 분배되는 성질을 보다 실용적으로 활용하여 지하수 TCE 오염에 대한 심도 있는 이해를 할 수 있음을 확인할 수 있었다.

주요어: 비활성기체, TCE, 분배, 추적자, 유기 오염 물질, 지하수 오염